JOURNAL OF AIRCRAFT
Vol. 30, No. 1, Jan.–Feb. 1993

Supersonic Flutter of Laminated Thin Plates with Thermal Effects

D. G. Liaw*
Sverdrup Technology, Inc., Brook Park, Ohio 44142

A 48 degree-of-freedom rectangular laminated thin plate finite element including the effects of thermal and aerodynamic loadings is formulated to study the buckling and supersonic flutter characteristics of thin plate structures. Interactive effects between the critical temperature difference and critical aerodynamic pressure for the plates are also studied. The element formulation is based on the classical lamination theory. The aerodynamic pressure due to supersonic potential flow is described by a two-dimensional steady supersonic theory. The element formulation and solution procedure are evaluated by comparing results of three examples with existing alternative solutions. The practical applicability is demonstrated by performing buckling and supersonic flutter analyses of laminated thin plates under various types of temperature distributions. Based on the numerical results, the effects of aspect ratio, ratio of thermal expansion coefficients, fiber orientation, type of temperature distribution, and flow angularity on these examples are discussed.

Introduction

THIN plates are a popular and useful form of structural components with significant applications in aerospace vehicles, such as high-speed aircraft, rocket, and spacecraft, which are subjected to thermal loads due to aerodynamic and/or solar radiation heating. This results in a temperature distribution over the surface and thermal gradient through the thickness of the plate. Due to boundary constraints, compressive stresses are induced and may cause buckling. Therefore, thermal buckling is a significant failure mode governing the design of thin plates used in aerospace structures.

For obvious advantages such as the high-strength-to-weight ratio and high-stiffness-to-weight ratio, etc., fiber-reinforced laminated composite materials have been increasingly used in the design and fabrication of thin plate structures.

It is of interest to briefly review the works done in thermal buckling of laminated composite plates. For example, Whitney and Ashton[1] studied the thermal buckling of symmetric, angle-ply, layered composite plates with simply supported edges using energy formulation. The critical temperatures for plates with various types of composite were presented. Chen and Chen[2] analyzed the thermal buckling of laminated cylindrical panels using Galerkin's method. The critical temperatures for plates with various structural and material parameters, and boundary conditions were presented. Tauchert and Huang[3] investigated thermal buckling of simply supported symmetric angle-ply laminated plates under uniform temperature change using the Rayleigh-Ritz method. The critical temperature and associated mode shape for plates with various fiber orientations, numbers of layers, and aspect ratios were presented. Thangaratnam et al.[4] studied the thermal buckling of composite laminated plates using semiloof finite elements. The critical temperatures for plates under various types of temperature distribution, lamination parameters, and boundary conditions were presented. Chen and Chen[5] analyzed the thermal buckling of laminated cylindrical plates subjected to a nonuniform temperature field using the finite element method. The critical temperatures for the plates with various lamination angle, modulus ratio, number of layers, plate aspect ratio, and boundary condition were presented.

In addition to buckling, supersonic flutter is another significant failure mode considered in the design of structural components for aerospace vehicles. Flutter of a panel in the supersonic flow falls in the category of self-excited oscillations. Small amplitude linear structural theory indicates that there is a critical dynamic pressure value above which the panel motion becomes unstable and grows exponentially with time.

The problem of supersonic flutter of composite plates has been extensively studied due to the increased use of composite materials in aerospace application. The outline of such study was given by Librescu[6] in an excellent, thorough, and definitive monograph. It is also of interest to briefly review the works done in this field by other investigators. For example, Rossettos and Tong[7] studied the effects of filament angle and orthotropicity parameter on the flutter characteristics of cantilevered anisotropic plates using the hybrid stress finite element method. Sawyer[8] developed an anisotropic analysis and solution procedure using linear small-deflection theory for flutter of finite, simply-supported general laminated plates with arbitrary fiber orientations. The extended Galerkin's method was used to obtain approximate solutions to the coupled governing equations. Ramkumar and Weisshaar[9] studied the supersonic flutter characteristics of flat rectangular anisotropic plates composed of advanced composite materials using the Rayleigh-Ritz method. The effects of the orientation of the ply material principal axes, the number of plies, and the aspect ratio of the plate were investigated. Chatterjee and Kulkarni[10] studied the effects of environment, damping, and shear deformations on the flutter characteristics of laminated composite panels using the Rayleigh-Ritz method. Oyibo[11] analyzed the flutter problems of rectangular simply supported orthotropic panels subjected to supersonic flow over one surface using affine transformations in the analysis, and using the Galerkin method in solving the equations of motion. Srinivasan and Babu[12] investigated the flutter characteristics of laminated quadrilateral plates with clamped edges. Differential equations of motion in quadrilateral coordinates were derived and solved using the integral equation technique. Lin et al.[13,14] studied the panel flutter of composite thin plates in the supersonic flow and subsonic flow using 18-degree-of-freedom triangular thin plate finite elements. The effects of composite filament angle, orthotropic modulus ratio, sweep angle, and aspect ratio on the flutter characteristics were investigated.

It appears that in most former studies, the phenomena of thermal buckling and supersonic flutter were investigated sep-

Received April 3, 1991; revision received Oct. 18, 1991; accepted for publication Jan. 20, 1992.

*Senior Engineer, NASA Lewis Research Center Group. Member AIAA.

arately. However, it is important and desirable to consider the interactive effects of both failure characteristics in the analysis, design, and safety assessment of practical aerospace structures simultaneously. Therefore, it appears timely to formulate a laminated thin plate finite element including both thermal and aerodynamic effects to study the supersonic flutter behavior of general laminated thin plates subjected to thermal loads.

The author has formulated a 16-degree-of-freedom rectangular thin plate finite element to investigate the supersonic flutter behavior of laminated plate structures.[15] It is the intent of this study to extend this earlier formulation to include the thermal effect to study the thermal buckling and supersonic flutter of laminated plates simultaneously.

In this study, the plate is assumed to be thin so that the classical lamination theory is applicable. The aerodynamic pressure due to supersonic potential flow is described by the two-dimensional quasisteady supersonic theory which is also called piston theory.[16] The structural and aerodynamic dampings have a significant effect on the determination of the flutter characteristics. Such effect has been studied previously by, among others, Librescu and Badoiu[17] and Librescu.[6] However, the effects of structural and aerodynamic dampings are not considered in this article. In such a case, a steady rather than a quasisteady aerodynamic supersonic theory is used. Consequently, the frequency coalescence technique can be used to determine the flutter boundary. When the damping effects are considered, other methods, such as the stability parabola concept coupled with the Sylvester determinant technique, have to be used to determine the flutter instability. The aforementioned method was described and used to deal with such problems in Ref. 6.

For the purpose of more practical applications, the temperature distribution is considered to be various both over the surface and through the thickness. It is a well-known fact that at the level of temperatures occurring at supersonic speeds, there is a degradation of the elastic properties of the constituent materials which is a function of the temperature field itself. Such an effect is not considered in this article. It is also known that the buckling load of a plate in the presence of the airflow is higher than in the case of its absence.[6] Such a stabilizing effect is also not considered in this article.

To evaluate the validity of the present finite element formulation and solution procedure, three examples were studied for which alternative solutions are available for comparison: 1) a thermal buckling analysis of cross-ply laminated plates with various ratios of thermal expansion coefficients and aspect ratios; 2) a supersonic flutter analysis of symmetric angle-ply laminated plates with various aspect ratios and fiber orientations; and 3) a supersonic flutter analysis of antisymmetric angle-ply laminated plates with various fiber orientations and flow angularities. To demonstrate the practical applicability of the present developments, three more examples were studied: 1) supersonic flutter of isotropic square plates under uniaxial and biaxial in-plane loads; 2) supersonic flutter of laminated square plates under uniaxial in-plane loads; and 3) thermal buckling and supersonic flutter of laminated rectangular plates with various fiber orientations and types of temperature distribution.

Based on the numerical results, the effects of fiber orientation, aspect ratio, ratio of thermal expansion coefficients, type of temperature distribution, and flow angularity on the buckling and supersonic flutter of laminated plate structures are discussed.

Formulation

An earlier finite element formulation developed by the author for buckling and supersonic flutter analyses of laminated thin plate structures is extended here to include the effects of aerodynamic and thermal loads simultaneously.[15] The rectangular element possesses 12 DOF at each of the four corner nodes: u, u_x, u_y, u_{xy}, v, v_x, v_y, v_{xy}, w, w_x, w_y, and w_{xy}, where u, v, and w are the displacements in the Cartesian coordinate system x, y, z, respectively. The subscript indicates differentiation.

Equations of Motion

The equations of motion for a thin elastic plate element may be derived using the Hamilton's principle. The element equations of motion can be obtained as

$$[m]\{\ddot{q}\} + ([k_L] + [k_{NL}] + [k_\sigma] + \lambda[a])\{q\} = \{0\} \quad (1)$$

where $[m]$, $[k_L]$, $[k_{NL}]$, $[k_\sigma]$, and $[a]$ are the consistent mass, linear stiffness, initial displacement, initial stress, and aerodynamic matrices, respectively. The aerodynamic parameter λ is defined as

$$\lambda = \frac{2\bar{q}}{\sqrt{M_\infty^2 - 1}} \quad (2)$$

where $\bar{q}$ is the aerodynamic pressure and M_∞ is the Mach number. Equation (1) can also be written as

$$[m]\{\ddot{q}\} + ([k_T] + \lambda[a])\{q\} = \{0\} \quad (3)$$

The matrix $[k_T]$ is called the tangential stiffness matrix and is written as

$$[k_T] = \iint_A [B_L + B_{NL}(q)]^T \begin{bmatrix} A & B \\ B & D \end{bmatrix} [B_L + B_{NL}(q)]\, dA + \iint_A [G]^T[H][G]\, dA \quad (4)$$

The matrices $[B_L]$ and $[B_{NL}(q)]$ relate the incremental strains $\{d\varepsilon\}$ to the incremental displacements $\{dq\}$ as

$$\{d\varepsilon\} = [B_L + B_{NL}(q)]\{dq\} \quad (5)$$

where $[B_L]$ is the same as that for the linear case. The strain-displacement matrix due to the geometrically nonlinear effect is $[B_{NL}]$. The coefficients in the laminate constitutive matrices $[A]$, $[B]$, and $[D]$ are given as

$$[A_{ij}, B_{ij}, D_{ij}] = \int_{-h/2}^{h/2} Q_{ij}(1, z, z^2)\, dz \qquad (i, j = 1, 2, 6) \quad (6)$$

with Q_{ij} denoting the plane-stress stiffness for an individual layer and h the total thickness of the plate. The matrix $[G]$ relates the first derivatives of displacements to the element degrees of freedom as

$$\{u_x, v_x, w_x, u_y, v_y, w_y\}^T = [G]\{q\} \quad (7)$$

Thus $[G]$ is a matrix defined purely in terms of the coordinates. The matrix $[H]$ is given as

$$[H] = \begin{bmatrix} N_x & 0 & 0 & N_{xy} & 0 & 0 \\ 0 & N_x & 0 & 0 & N_{xy} & 0 \\ 0 & 0 & N_x & 0 & 0 & N_{xy} \\ N_{xy} & 0 & 0 & N_y & 0 & 0 \\ 0 & N_{xy} & 0 & 0 & N_y & 0 \\ 0 & 0 & N_{xy} & 0 & 0 & N_y \end{bmatrix} \quad (8)$$

where the thermal forces, N_x, N_y, and N_{xy}, are defined as

$$\begin{Bmatrix} N_x \\ N_y \\ N_{xy} \end{Bmatrix}_k = \int_{-h/2}^{h/2} \Delta T(z)[Q] \begin{Bmatrix} \alpha_x \\ \alpha_y \\ \alpha_{xy} \end{Bmatrix} dz \quad (9)$$

with α_{ij} $(i, j = x, y)$ denoting the thermal expansion coeffi-

cients in the global coordinates, and ΔT the temperature difference.

The aerodynamic pressure due to supersonic potential flow is described by the two-dimensional quasisteady supersonic theory as

$$p(x, y, t) = \lambda \left(\frac{\partial w}{\partial \xi} + \frac{1}{V} \frac{M_\infty^2 - 2}{M_\infty^2 - 1} \frac{\partial w}{\partial t} \right) \tag{10}$$

where V is the flow velocity and ξ is the direction of the flow in the global coordinate system. The aerodynamic damping has an effect on the determination of the flutter characteristics. The effect is not considered here. In such a case, a steady rather than the quasisteady aerodynamic supersonic theory is used. By following the procedure proposed by Sander et al.[18] and Yang,[19] the explicit form for the coefficient in the aerodynamic matrix can be obtained as the following general form:

$$a_{ij} = \lambda \int_A N_i \frac{\partial N_j}{\partial \eta} \frac{\partial \eta}{\partial \xi} \, dA \tag{11}$$

where N_i is the shape function for the ith DOF and η is the direction of the flow in the local element coordinates.

It is noted that in this study the geometric nonlinearity is not considered. Therefore, the initial displacement matrix $[k_{NL}]$ is assumed to be zero.

By assembling the finite elements for the entire plate system and applying the kinematic conditions, the equations of motion for the entire system can be expressed in the same form as Eq. (1) by capitalizing all the symbols

$$[M]\{\ddot{Q}\} + ([K_L] + \Delta T[\bar{K}_\sigma] + \lambda[A])\{Q\} = \{0\} \tag{12}$$

Solution Procedure

In order to solve Eq. (12), the displacement vector is assumed as an exponential function of time as

$$\{\ddot{Q}\} = \{Q\} e^{\Omega t} \tag{13}$$

where Ω is a complex number. By substituting Eq. (13) into Eq. (12), the equations of motion become

$$(\Omega^2[M] + [K_L] + \Delta T[\bar{K}_\sigma] + \lambda[A])\{Q\} = \{0\} \tag{14}$$

Equation (14) represents a general eigenvalue problem. For $\lambda = 0$ and $\Omega = 0$, the problem degenerates into that of finding the critical temperature difference (ΔT_{cr}) of the plate in the thermal buckling analysis. For $\lambda = 0$ and $\Delta T = 0$, the problem degenerates into that of finding the free vibration frequencies of the plate in vacuo. In the general and practical cases, at a given temperature difference ($\Delta T \neq 0$), when the aerodynamic pressure λ is increased from zero, two eigenvalues will usually approach each other and coalesce to Ω_{cr} at $\lambda = \lambda_{cr}$ and become a complex conjugate pair for $\lambda > \lambda_{cr}$. Here λ_{cr} is considered to be that value of λ at which first coalescence occurs for a specific temperature difference ΔT.

Results

To evaluate the validity and to demonstrate the practical applicability of the present finite element formulation and solution procedure, a series of thermal buckling and supersonic flutter analyses of laminated thin plates were performed. Interactive effect between the critical temperature difference and aerodynamic pressure was also studied.

In all examples, a sufficiently fine Gauss grid (5 × 5) was used for numerical integration to obtain the element stiffness, initial stress, mass, and aerodynamic matrices. This mesh was shown numerically to be sufficiently fine for all the present examples, i.e, this mesh yielded converged results as it was successively refined. All calculations were carried out using a CYBER 205 vectorized supercomputer at Purdue University.

Thermal Buckling of Symmetric Cross-Ply Laminated Plates

The example rectangular plates studied were assumed to be simply supported with a length $a = 100$ in. The laminate construction was assumed as [0/90/90/0] with thickness of each lamina equal to 0.25 in. The material of each lamina was assumed as a graphite/epoxy with the following properties: $E_L = 20$ msi, $E_T = 1.0$ msi, $G_{LT} = 0.5$ msi, $\nu_{LT} = 0.25$, and $\alpha_L = 1.0 \times 10^{-6}$ in./in./°F.

The effects of aspect ratio (a/b) and ratio of thermal expansion coefficients (α_T/α_L) on the critical temperature difference were investigated in this example. The ranges for the aspect ratio and ratio of thermal expansion coefficients were considered between 0.1–5, and between 0–20, respectively.

Due to symmetry, only a quadrant of the plate was modeled using a 2 × 2 mesh with appropriate boundary conditions. Figure 1 shows the results for critical temperature differences of plates with various aspect ratios and ratios of thermal expansion coefficients. The critical temperature differences for certain cases were obtained previously by Thangaratnam et al.[4] using semiloof finite elements. Their results are also plotted for comparison and excellent agreement is seen.

It is seen that for all cases possessing various ratios of thermal expansion coefficients, the critical temperature difference decreases from an aspect ratio 0–1 with a very slow rate, then increases from 1 to 5 with a faster rate. The critical temperature difference is minimum when the aspect ratio is equal to 1 (i.e., a simply supported square plate). It is also seen as expected that, when the ratio of thermal expansion coefficients increases, the critical temperature decreases for all values of aspect ratio.

Supersonic Flutter of Symmetric Angle-Ply Laminated Composite Rectangular Plates

The example rectangular plates studied were assumed as simply supported with a length $a = 100$ in. The laminate construction was assumed as $[\theta/-\theta/-\theta/\theta]$ with the thickness of each lamina equal to 0.25 in. The material of each lamina was assumed as a boron/epoxy with the following properties: $E_L = 30$ msi, $E_T = 3.0$ msi, $G_{LT} = 1.0$ msi, $\nu_{LT} = 0.3$, and $\rho = 0.145 \times 10^{-3}$ lb-s^2/in.^{4}

The effects of aspect ratio and fiber orientation θ on the critical aerodynamic pressure were investigated in this example. Three plates with different aspect ratios ($a/b = 0.5$, 1.0, and 2.0) were considered. The range for fiber orientation was taken between 0 and 90 deg.

A 4 × 4 finite element mesh was used to model the whole plate. Figure 2 shows the results for critical aerodynamic pres-

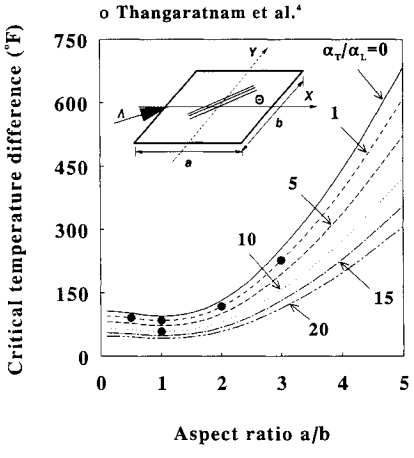

Fig. 1 Critical temperature difference of simply supported laminated [0/90/90/0] rectangular plates with various aspect ratios and ratios of thermal expansion coefficients.

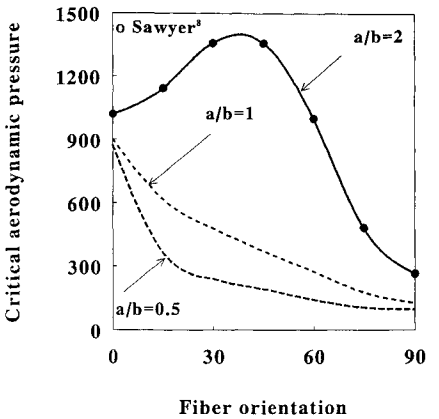

Fig. 2 Critical aerodynamic pressure of simply supported laminated $[\theta/-\theta/-\theta/\theta]$ rectangular plates with various fiber orientations and aspect ratios.

sure of the plates with various aspect ratios and fiber orientations. The critical aerodynamic pressure for the case of $a/b = 2$ was obtained previously by Sawyer[8] using the Galerkin method. His results are also plotted for comparison and excellent agreement is seen.

It is seen that, for the case of $a/b = 2$, the critical aerodynamic pressure increases when the fiber orientation varies from 0 to 40 deg, then decreases when the fiber orientation varies from 40 to 90 deg. The maximum and minimum critical aerodynamic pressures are obtained when the fiber orientations are about 40 and 90 deg, respectively. However, for the cases of $a/b = 1.0$ and 0.5, the critical aerodynamic pressure decreases monotonously when the fiber orientation varies from 0 to 90 deg. The maximum and minimum critical aerodynamic pressures are obtained when the fiber orientations are equal to 0 and 90 deg, respectively.

It is noted that, for the case of $a/b = 2$, the lowest two natural frequencies coalesce first. As a result, the supersonic flutter of the plate occurs. However, for the cases of $a/b = 1.0$ and 0.5, the first coalescence of the natural frequencies does not always occur in the lowest two natural frequencies, i.e, the flutter of the plate occurs in the higher modes. For example, in the case of $a/b = 1.0$ and $\theta = 15$ deg, the third and fourth modes coalesce first as seen in Fig. 3.

Supersonic Flutter of Antisymmetric Angle-Ply Laminated Composite Square Plates

The example square plates studied were assumed as simply supported with a length $a = b = 100$ in. The laminate construction was assumed as $[\theta/-\theta/\theta/-\theta]$ with the thickness of each lamina equal to 0.25 in. The material of each lamina was assumed as boron/epoxy with the same properties as those of the previous example.

For more practical applications, the direction of airflow over the plate surface will vary. Therefore, the effects of the direction of airflow on the critical aerodynamic pressure were investigated in this example. Four directions of airflow ($\Lambda = 0$, 15, 30, and 45 deg) were considered. The range for fiber orientation was taken between 0 and 90 deg.

A 4×4 finite element mesh was used to model the whole plate. Figure 4 shows the results for critical aerodynamic pressure of the plates with various fiber orientations in supersonic flow with various directions of airflow. The critical aerodynamic pressure for the case of $\Lambda = 15$ and 30 deg was obtained previously by Sawyer[8] using the Galerkin method. His results are also plotted for comparison and excellent agreement is seen.

It is seen that, for the case of $\Lambda = 0$ deg, the critical aerodynamic pressure decreases monotonously when the fiber orientation varies from 0 to 90 deg. However, for the cases of $\Lambda = 15$, 30, and 45 deg, the critical aerodynamic pressure increases when the fiber orientation varies from 0 to approximately 30, 40, and 45 deg, respectively, and then decreases.

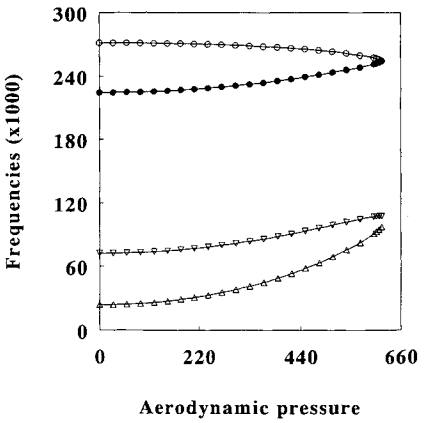

Fig. 3 Coalescence of the frequencies of the simply supported laminated [15/−15/−15/15] square plate.

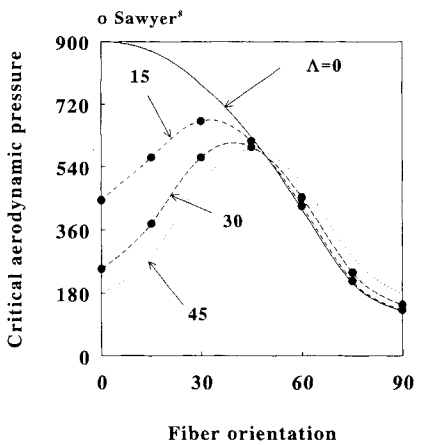

Fig. 4 Critical aerodynamic pressure of simply supported laminated $[\theta/-\theta/\theta/-\theta]$ rectangular plates with various fiber orientations and angles of airflow.

It is noted that aligning the fibers with the flow generally results in the highest aerodynamic pressure.

It is also noted that the results of the critical aerodynamic pressures in this square plate for flow angle $\Lambda = 60$, 75, and 90 deg are symmetric with the results for $\Lambda = 30$, 15, and 0 deg, respectively. In other words, the critical aerodynamic pressure for the plate with fiber orientation θ in the airflow with direction Λ is equal to that for the plate with fiber orientation 90-θ in the airflow with direction 90-Λ.

Supersonic Flutter of Isotropic Square Plates Under Uniaxial or Biaxial In-Plane Loads

The example square plates studied were assumed as simply supported or clamped with a length $a = b = 50$ in. and a thickness $h = 1$ in. The material properties were assumed as those for steel with $E = 30 \times 10^6$ psi, $\nu = 0.3$, and $\rho = 0.733 \times 10^{-3}$ lb-s^2/in.[4]

As a first step, buckling analysis of the plate was performed. A 4×2 finite element mesh was used to model half of the plate. The buckling loads for the simply supported plate under uniaxial ($N_x \neq 0$, $N_y = 0$) and biaxial ($N_x = N_y \neq 0$) in-plane loads are $(N_{cr})_u = 43.4 \times 10^3$ lb/in. and $(N_{cr})_{b1} = (N_{cr})_u/2 = 21.7 \times 10^3$ lb/in., respectively. In order to study the effect of in-plane load N_y on the critical aerodynamic pressure, another in-plane loading condition $N_y = N_x/2$ is also considered. The corresponding buckling load $(N_{cr})_{b2}$ is equal to $2(N_{cr})_u/3 = 28.9 \times 10^3$ lb/in. The comparison of these numerical solutions with the theoretical solutions is excellent.[20]

Figure 5 shows the results for the critical aerodynamic pressure of the simply supported plate under various in-plane loads. It is of interest to see that the critical aerodynamic pressure decreases from $(\lambda_{cr})_0$ when the in-plane load in-

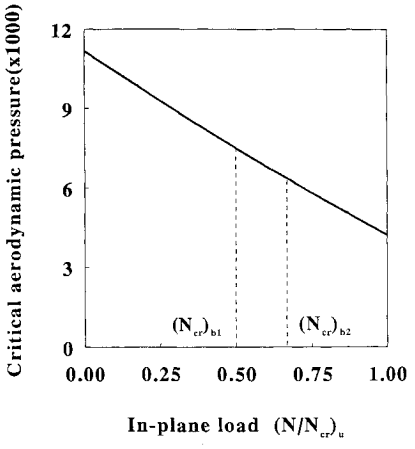

Fig. 5 Critical aerodynamic pressure of simply supported isotropic square plates under uniaxial and biaxial in-plane loads.

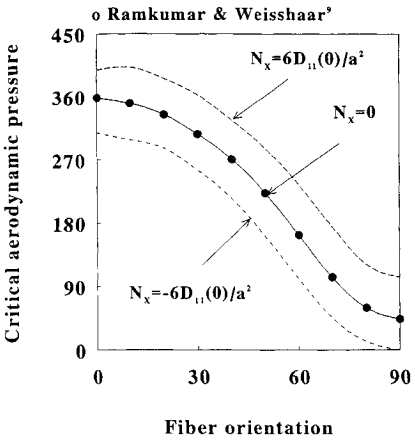

Fig. 6 Critical aerodynamic pressure of simply supported laminated $[\theta/-\theta]_{10S}$ rectangular plates with various fiber orientations under uniformly distributed in-plane loads.

creases from zero to N_{cr}. Here $(\lambda_{cr})_0$ is the critical aerodynamic pressure of the plate without in-plane load. The value of $(\lambda_{cr})_0$ ($=11.18$ ksi) obtained here is in a good agreement with that in Ref. 17. It is noted that the critical aerodynamic pressure is not equal to zero when the in-plane load is equal to N_{cr}. It is also interesting to see that the critical aerodynamic pressures for all cases are the same for a specific in-plane load N_x, but are not influenced by the in-plane load N_y.

Supersonic Flutter of Symmetric Angle-Ply Laminated Plates Under In-Plane Loads

The example square plates studied were assumed as simply supported with a length $a = 100$ in. The laminate construction was assumed as $[\theta/-\theta]_{10S}$ with thickness of each lamina equal to 0.05 in. The material of each lamina was assumed as a boron/epoxy with the following properties: $E_L = 30$ msi, $E_T = 2.7$ msi, $G_{LT} = 0.9$ msi, and $\nu_{LT} = 0.21$.

In the design of thin plate structures, such as a panel in a wing, it is often necessary to consider the effect of in-plane loads. Therefore, the effects of the in-plane loads on the critical aerodynamic pressure were investigated in this example. Three uniformly distributed uniaxial in-plane loads, $N_x = 6D_{11}(0)/a^2$, 0, $-6D_{11}(0)/a^2$, were considered. The symbol $D_{11}(0)$ represents the value of D_{11} when all fibers are aligned parallel to the airstream where D_{11} is the longitudinal bending stiffness of the plate. The range for fiber orientation was taken between 0–90 deg.

A 4×4 finite element mesh was used to model the whole plate. Figure 6 shows the results for critical aerodynamic pressure of the plates with various fiber orientations under uniformly distributed in-plane loads. The critical aerodynamic pressure for the case of $N_x = 0$ was obtained previously by Ramkumar and Weisshaar[9] using the Rayleigh-Ritz method. Their results are also plotted for comparison and excellent agreement is seen.

It is seen that the critical aerodynamic pressure decreases when the fiber orientation varies from 0 to 90 deg for all three cases. It is also seen that the in-plane tension has an effect on increasing the critical aerodynamic pressure. On the other hand, the in-plane compression has an effect on decreasing the critical aerodynamic pressure. The beneficial effect of in-plane tension and the detrimental effect of in-plane compression have also been observed previously by, among others, Hedgepeth,[21] Bisplinghoff and Ashley,[16] and Dugundji[22] for isotropic two-dimensional panels and by Librescu[6] for orthotropic plates.

Thermal Buckling and Supersonic Flutter of Simply Supported Laminated Composite Rectangular Plates with Various Temperature Distributions

The example rectangular plates studied were assumed as simply supported with a length $a = 100$ in. and a width $b = 50$ in. The laminate construction was assumed as $[\theta/-\theta/-\theta/\theta]$ with the thickness of each lamina equal to 0.25 in. The material of each lamina was assumed as a boron/epoxy with the following properties: $E_L = 30$ msi, $E_T = 3.0$ msi, $G_{LT} = 1.0$ msi, $\nu_{LT} = 0.3$, $\rho = 0.145 \times 10^{-3}$ lb-s^2/in.^{4}, $\alpha_L = 1.0 \times 10^{-6}$ in/in/F, and $\alpha_T = 2.0 \times 10^{-6}$ in/in/F.

The effects of the type of temperature distribution and fiber orientation on the critical temperature difference and critical aerodynamic pressure were investigated in this example. The temperature field considered in this example is described as the following general form:

$$T(x, y, z) = T_{\max} T_{xy}(x, y) T_z(z) \tag{15}$$

where $T_{\max}$ is the highest temperature in the field, and T_{xy} and T_z are the temperature distribution functions along the plane of the plate and through the thickness, respectively. Two kinds of temperature distributions along the plane of the plate were assumed. These were uniform distribution $[T_{xy}(x, y) = 1]$ and sinusoidal distribution $\{T_{xy}(x, y) = \sin[\pi(x + a/2)/a]\sin[\pi(y + b/2)/b]\}$. On the other hand, two kinds of distributions through the thickness were assumed. These were uniform distribution $[T_z(z) = 1]$ and linear distribution $[T_z(z) = 0.5 + z/h]$. By combining the previously mentioned horizontal and transverse temperature distributions together, four types of temperature distributions were obtained as shown in Table 1 and used in this example. The range for fiber orientation was taken between 0 and 90 deg.

As a first step, thermal buckling analysis of the plate was performed. A 4×4 finite element mesh was used to model the whole plate. Figure 7 shows the results for critical temperature difference of the plate under various temperature distributions. It is of interest to see that the critical temperature differences for temperature distribution type 2 are twice of those for temperature distribution type 1 because the magnitude of the total in-plane load for type 1 is twice of that for type 2. Similarly, it is seen that the critical temperature differences for temperature distribution type 4 are twice of those for type 3 due to the same reason.

It is also seen that the critical temperature differences for types 3 and 4 are 2.4674 ($=\pi^2/4$) times of those for types 1

Table 1 Definition of the temperature distributions used in example 6

Type	Horizontal direction $T_{xy}(x, y)$	Transverse direction $T_z(z)$
1	1	1
2	1	$0.5 + (z/h)$
3	$\sin[\pi(x + a/2)/a]\sin[\pi(y + b/2)/b]$	1
4	$\sin[\pi(x + a/2)/a]\sin[\pi(y + b/2)/b]$	$0.5 + (z/h)$

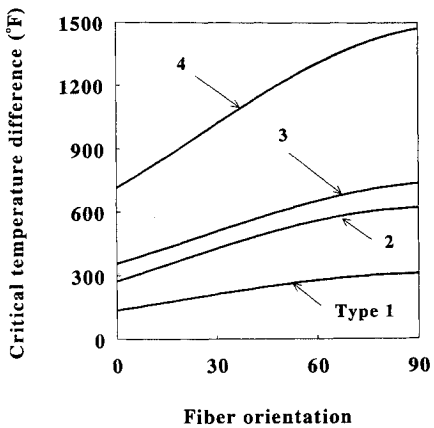

Fig. 7 Critical temperature difference of simply supported laminated [θ/−θ/−θ/θ] rectangular plates with various fiber orientations and temperature distributions.

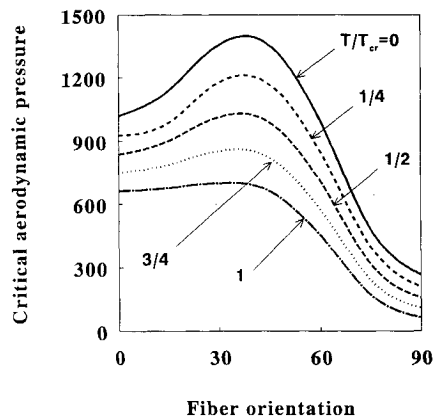

Fig. 8 Critical aerodynamic pressure of simply supported laminated [θ/−θ/−θ/θ] rectangular plates with various fiber orientations and temperature differences of temperature distribution types 1 and 2.

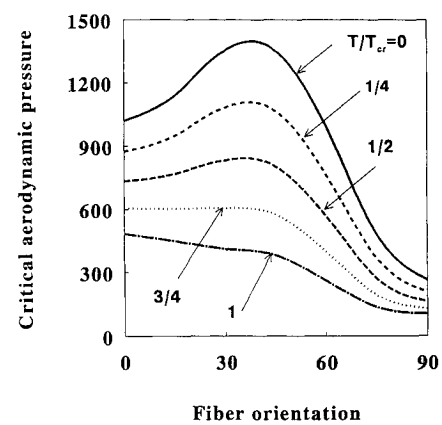

Fig. 9 Critical aerodynamic pressure of simply supported laminated [θ/−θ/−θ/θ] rectangular plates with various fiber orientations and temperature differences of temperature distribution types 3 and 4.

and 2, respectively, because the magnitude of the total in-plane load for types 1 and 2 is 2.4674 times of that for types 3 and 4, respectively. Although the critical temperature differences for types 2, 3, and 4 can be calculated theoretically using the results for type 1, the advantage of this finite element approach exists in predicting the critical temperature difference for practical structures with complex temperature distribution in both horizontal and transverse directions.

Figure 8 shows the results for the critical aerodynamic pressure of the plate with various fiber orientations under temperature distribution type 1. Five nondimensional values of temperature differences were considered (T/T_{cr} = 0, ¼, ½, ¾, and 1). It is noted that the results shown in Fig. 8 are also applicable for the plate under temperature distribution type 2. However, the critical temperature differences (T_{cr}) for types 1 and 2 are different. As shown in Fig. 7, the critical temperature difference for type 2 is twice of that for type 1.

Figure 9 shows the results for the critical aerodynamic pressure of the plate with various fiber orientations under temperature distribution types 3 and 4 with five values of temperature difference (T/T_{cr} = 0, ¼, ½, ¾, and 1).

It is seen that (in Figs. 8 and 9) the temperature difference has an obvious effect on reducing the critical aerodynamic pressure. Such effect is most pronounced when the angle between the fiber orientation and airflow is around 40 deg.

It is also seen in most cases studied that when the fiber orientation varies from 0 to 90 deg, the critical aerodynamic pressure increases and reaches a peak value when the fiber orientation is around 40 deg, then decreases. The rate of increase becomes less obvious when the temperature difference increases.

Concluding Remarks

A 48 degree-of-freedom rectangular laminated thin plate finite element with the effects of thermal and aerodynamic loads has been formulated. A numerical solution procedure for thermal buckling and supersonic flutter analyses has also been developed.

The validity of the present formulation is established through comparison of the present results with existing alternative solutions. The applicability is demonstrated by performing a series of thermal buckling and supersonic flutter analyses of laminated thin plate structures.

The present numerical results show that the aspect ratio, ratio of thermal expansion coefficients, fiber orientation of the plate, type of temperature distribution, and flow angularity, have an obvious effect on the critical temperature difference and critical aerodynamic pressure of laminated plates.

Moreover, the present element formulation and solution procedure provide a useful tool for studying the supersonic flutter behavior of practical laminated plate structures subjected to thermal loads with complex temperature distributions.

The present formulation and solution procedure are general and simple so that extensions can be made to include some more interesting effects, such as transverse shear deformations for thick plates, structural and aerodynamic dampings, temperature-dependent material properties, as well as structural and aerodynamic nonlinearities.

Acknowledgments

The primary portion of this work was done when the author was a graduate student in Purdue University. The author is grateful to his major professor, Henry T. Y. Yang, for his initial and continual guidance on this work. The author expresses his gratitude to the reviewers for their helpful and useful comments and suggestions on the original manuscript.

References

[1]Whitney, J. M., and Ashton, J. E., "Effect of Environment on the Elastic Response of Layered Composite Plate," *AIAA Journal*, Vol. 7, No. 9, 1971, pp. 1708–1713.

[2]Chen, L. N., and Chen, L. Y., "Thermal Buckling of Laminated Cylindrical Plates," *Composite Structures*, Vol. 8, No. 3, 1987, pp. 189–205.

[3]Tauchert, T. R., and Huang, N. N., "Thermal Buckling of Symmetric Angle-Ply Laminated Plates," *Proceedings of the 4th International Conference on Composite Structures*, Elsevier, Barking, England, UK, 1987, pp. I.424–I.435.

[4]Thangaratnam, K. R., Pallaninathan, R., and Ramachandran, J., "Thermal Buckling of Composite Laminated Plates," *Computers and Structures*, Vol. 32, No. 5, 1989, pp. 1117–1124.

[5]Chen, L. W., and Chen, L. Y., "Thermal Buckling Analysis of Laminated Cylindrical Plates by the Finite Element Method," *Com-*

puters and Structures, Vol. 34, No. 1, 1990, pp. 71–78.
[6]Librescu, L., *Elastostatics and Kinetics of Anisotropic and Heterogeneous Shell-Type Structures*, 1st ed., Noordhoff, Leyden, The Netherlands, 1975.
[7]Rossettos, J. N., and Tong, P., "Finite-Element Analysis of Vibration and Flutter of Cantilever Anisotropic Plates," *Journal of Applied Mechanics*, Vol. 41, No. 4, 1974, pp. 1075–1080.
[8]Sawyer, J. W., "Flutter and Buckling of General Laminated Plates," *Journal of Aircraft*, Vol. 14, No. 4, 1977, pp. 387–393.
[9]Ramkumar, R. L., and Weisshaar, T. A., "Flutter of Flat Rectangular Plates in High Mach Number Supersonic Flow," *Journal of Sound and Vibration*, Vol. 50, No. 4, 1977, pp. 587–597.
[10]Chatterjee, S. N., and Kulkarni, S. V., "Effects of Environment, Damping and Shear Deformations on Flutter of Laminated Composite Panels," *International Journal of Solids and Structures*, Vol. 15, No. 6, 1979, pp. 479–491.
[11]Oyibo, G. A., "Flutter of Orthotropic Panels in Supersonic Flow Using Affine Transformations," *AIAA Journal*, Vol. 21, No. 2, 1983, pp. 283–289.
[12]Srinivasan, R. S., and Babu, B. J. C., "Free Vibration and Flutter of Laminated Quadrilateral Plates," *Computers and Structures*, Vol. 27, No. 2, 1987, pp. 297–304.
[13]Lin, K. J., Lu, P. J., and Tarn, J. Q., "Flutter Analysis of Composite Panels Using High-Precision Finite Elements," *Computers and Structures*, Vol. 33, No. 2, 1989, pp. 561–574.
[14]Lin, K. J., Lu, P. J., and Tarn, J. Q., "Flutter Analysis of Cantilever Composite Panels in Subsonic Flow," *AIAA Journal*, Vol. 27, No. 8, 1989, pp. 1102–1109.
[15]Liaw, D. G., and Yang, H. T. Y., "Reliability of Initially Compressed Uncertain Laminated Plates in Supersonic Flow," *AIAA Journal*, Vol. 29, No. 6, 1991, pp. 952–960.
[16]Bisplinghoff, R. L., and Ashley, H., *Principles of Aeroelasticity*, 1st ed., Wiley, New York, 1962.
[17]Librescu, L., and Badoiu, T., "On the Supersonic Flutter of Rectangular, Anisotropic, Heterogeneous Flat Structures," NASA-TT-F-15890, 1974.
[18]Sander, G., Bon, C., and Geradin, M., "Finite Element Analysis of Supersonic Panel Flutter," *International Journal for Numerical Methods in Engineering*, Vol. 7, No. 3, 1973, pp. 379–394.
[19]Yang, T. Y., "Flutter of Flat Finite Element Panels in Supersonic Unsteady Potential Flow," *AIAA Journal*, Vol. 13, No. 11, 1975, pp. 1502–1507.
[20]Timoshenko, S., and Woinowsky-Krieger, S., *Theory of Plates and Shells*, 2nd ed., McGraw-Hill, New York, 1959.
[21]Hedgepeth, J. M., "Flutter of Rectangular Simply Supported Panels at High Supersonic Speeds," *Journal of Aeronautical Sciences*, Vol. 24, No. 8, 1957, pp. 563–573.
[22]Dugundji, J., "Theoretical Considerations of Panel Flutter at High Supersonic Mach Numbers," *AIAA Journal*, Vol. 4, No. 7, 1966, pp. 1257–1266.